

Theoretical and experimental study of the Suzuki-phase photonic crystal lattice by angle-resolved photoluminescence spectroscopy

Alfonso Rodríguez Alija, Luis Javier Martínez, and Pablo Aitor Postigo

Instituto de Microelectrónica de Madrid (CNM, CSIC), Isaac Newton 8, E-28760, Tres Cantos Madrid, Spain.

alija@imm.cnm.csic.es

Jose Sánchez-Dehesa

Wave-Phenomena Group, Nanophotonics Technology Center and Department of Electronic Engineering, Polytechnic University of Valencia, Valencia E-46022, Spain

jsdehesa@upvnet.upv.es

Matteo Galli, Alberto Politi, Maddalena Patrini, and Lucio Claudio Andreani

Dipartimento di Fisica "A. Volta", Università di Pavia, via Bassi 6, I-27100 Pavia, Italy

galli@fisicavolta.unipv.it

Christian Seassal and Pierre Viktorovitch

Laboratoire d'Electronique, Optoélectronique et Microsystèmes, UMR CNRS 5512, Ecole Centrale de Lyon 36, avenue Guy de Collongue, BP 163, F-69131 Ecully Cedex, France

Christian.Seassal@ec-lyon.fr

Abstract: A complete theoretical and experimental analysis of the photonic band structure for the Suzuki-phase lattice is presented. The band diagrams were calculated by two-dimensional plane wave expansion and three-dimensional guided-mode expansion methods. Angle resolved photoluminescence spectroscopy has been used to measure the emission of the photonic crystal structure realized in active InAsP/InP slabs. Photonic bands with a very low group velocity along an entire direction of the reciprocal lattice have been measured, which may have important applications on future photonic devices. The experimentally determined dispersion is in very good agreement with the calculated photonic bands. The presence of defect modes produced by microcavities in the Suzuki-phase lattice has also been established.

© 2006 Optical Society of America

OCIS codes: (250.0250) Optoelectronics; (250.5300) Photonic integrated circuits; (250.5230) Photoluminescence

References and links

1. E. Yablonovitch, "Inhibited spontaneous emission in solid-state physics and electronics," *Phys. Rev. Lett.* **58**, 2059-2062 (1987).
2. S. John, "Strong localization of photons in certain disordered dielectric superlattices," *Phys. Rev. Lett.* **58**, 2486-2489 (1987).
3. J. D. Joannopoulos, R. D. Meade, and J. N. Winn, *Photonic Crystals* (Princeton University Press, Princeton, 1995).
4. S. Noda and T. Baba, *Roadmap on Photonic Crystals*, (Kluwer Academic Publishers, Dordrecht, 2003).
5. K. Inoue and K. Ohtaka, *Photonic Crystals: Physics, Fabrication and Applications* (Springer-Verlag, New York, 2004).
6. T. Asano, B. -S. Song, and S. Noda, "Analysis of the experimental Q factors (~ 1 million) of photonic crystal nanocavities," *Opt. Express* **14**, 1996-2002 (2006). <http://www.opticsinfobase.org/abstract.cfm?URI=oe-14-5-1996>.
7. H. Altug, D. Englund, and J. Vuckovic, "Ultrafast photonic crystal nanocavity laser," *Nat. Phys.* **2**, 484-488 (2006).
8. K. Nozaki and T. Baba, "Laser characteristics with ultimate-small modal volume in photonic crystal slab point-shift nanolasers," *Appl. Phys. Lett.* **88**, 211101 (2006).
9. T. Baba, N. Fukaya, and Yonekura, "Observation of light propagation in photonic crystal optical waveguides with bends," *Electron. Lett.* **35**, 654-656 (1999).
10. A. Chutinan and S. Noda, "Waveguides and waveguide bends in two-dimensional photonic crystal slabs," *Phys. Rev. B* **62**, 4488-4492 (2000).
11. M. Loncar, D. Nedeljkovic, T. Doll, J. Vuckovic, A. Scherer, and T. P. Pearsall, "Waveguiding in planar photonic crystals," *Appl. Phys. Lett.* **77**, 1937-1939 (2000).
12. M. Notomi, K. Yamada, A. Shinya, J. Takahashi, C. Takahashi, and I. Yokohama, "Extremely Large Group-Velocity Dispersion of Line-Defect Waveguides in Photonic Crystals Slabs," *Phys. Rev. Lett.* **87**, 253902 (2001).
13. S. McNab, N. Moll, and Y. Vlasov, "Ultra-low loss photonic integrated circuit with membrane-type photonic crystal waveguides," *Opt. Express* **11**, 2927-2939 (2003). <http://www.opticsinfobase.org/abstract.cfm?URI=oe-11-22-2927>.
14. Yurii A. Vlasov, Martin O'Boyle, Hendrik F. Hamann, and Sharee J. McNab, "Active control of slow light on a chip with photonic crystal waveguides," *Nature (London)* **438**, 65-69 (2005).
15. H. Altug and J. Vuckovic, "Experimental demonstration of the slow group velocity of light in two-dimensional coupled photonic crystal microcavity arrays," *Appl. Phys. Lett.* **86**, 111102 (2005).
16. C. Monat, C. Seassal, X. Letartre, P. Regreny, P. Rojo-Romeo, P. Viktorovitch, M. Le Vassor d'Yerville, D. Cassagne, J. P. Albert, E. Jalaguier, S. Pocas, and B. Aspar, "InP based 2-D photonic crystal on silicon: In-plane Bloch mode laser," *Appl. Phys. Lett.* **81**, 5102-5104 (2002).
17. X. Letartre, C. Monat, C. Seassal, and P. Viktorovitch, "Analytical modeling and an experimental investigation of two-dimensional photonic crystals microlasers: defect state (microcavity) versus band-edge state (distributed feedback) structures," *J. Opt. Soc. Am. B* **22**, 2581-2595 (2005).
18. D. Caballero, J. Sánchez-Dehesa, R. Martínez-Sala, C. Rubio, J.V. Sanchez-Perez, C. Rubio, L. Sanchis, and F. Meseguer, "Suzuki phase in two-dimensional sonic crystals," *Phys. Rev. B* **64**, 064303 (2001).
19. J. Sánchez-Dehesa, F. Ramos-Mendieta, J. Bravo-Abad, J. Martí, A. Martínez, and A. García, "Suzuki phase in two-dimensional photonic crystals," in *Photonic Bandgap Materials and Devices*, Ali Adibi, Axel Scherer, Shawn-Yu Lin, eds, *Proc. SPIE* **4655**, 251-259 (2002).
20. A. L. Reynolds, U. Perschel, F. Lederer, P. J. Roberts, T. F. Krauss, and P. J. I. de Maagt, "Coupled Defects in Photonic Crystals," *IEEE Trans. Microwave Theory Tech.*, **49**, 1860-1867 (2001).
21. L. C. Andreani, and D. Gerace, "Photonic-crystal slabs with a triangular lattice of triangular holes investigated using a guided-mode expansion method," *Phys. Rev. B* **73**, 235114 (2006).
22. A. R. Alija, L. J. Martínez, P. A. Postigo, C. Seassal, and P. Viktorovitch, "Coupled-cavity two-dimensional photonic crystal waveguide ring laser," *Appl. Phys. Lett.* **89**, 101102 (2006).
23. V. N. Astratov, D. M. Whittaker, I. S. Culshaw, R. M. Stevenson, M. S. Skolnick, T. F. Krauss, and R. M. De La Rue, "Photonic band-structure effects in the reflectivity of periodically patterned waveguides," *Phys. Rev. B* **60**, R16255 (1999).
24. A. David, C. Meier, R. Sharma, F.S. Diana, S.P. DenBaars, E. Hu, S. Nakamura, C. Weisbuch, and H. Benisty, "Photonic bands in two-dimensionally patterned multimode GaN waveguides for light extraction," *Appl. Phys. Lett.* **87**, 101107 (2005).
25. K. Sakai, E. Miyai, T. Sakaguchi, D. Ohnishi, T. Okano, and S. Noda, "Lasing band-edge identification for a surface-emitting photonic crystal laser," *IEEE J. Sel. Areas Commun.* **23**, 1335

- (2005).
26. M. Galli, A. Politi, M. Belotti, D. Gerace, M. Liscidini, M. Patrini, L. C. Andreani, M. Miritello, A. Irrera, F. Priolo, and Y. Chen, "Strong enhancement of Er^{3+} emission at room temperature in silicon-on-insulator photonic crystal waveguides," *Appl. Phys. Lett.* **88**, 251114 (2006).
 27. C. Monat, C. Seassal, X. Letartre, P. Regreny, P. Rojo-Romeo, P. Viktorovitch, M. Le Vassor d'Yerville, D. Cassagne, J.P. Albert, E. Jalaguier, S. Pocas, and B. Aspar, "Modal analysis and engineering of InP-based two-dimensional photonic crystal microlasers on a silicon wafer," *IEEE J. Quantum Electron.* **39**, 419-425 (2003).

1. Introduction

Since E. Yablonovitch [1] and S. John [2] opened the path of new advantageous structures, named photonic crystals (PC) [3-5], a large effort has been done in order to improve their quality and integrate them into the future photonic circuits. In particular, PC structures which present high quality factors [6], low thresholds [7] and small modal volume [8], are being studied in depth. Moreover, certain structures were proposed as promising components of devices for guiding light through a particular direction [9-11].

A very interesting feature of light guided through photonic crystals is that the group velocity of the light may be reduced by orders of magnitude. There are several devices taking advantage of this property both in PC waveguides [12-14] and in extended photonic crystal lattices [15-17]. In this case the light is not guided through any specific direction and the area for slow light is extended along the full photonic crystal structure. These photonic structures use also the high interaction of light with matter for laser emission.

In this paper we propose and measure the photonic band structure of the two dimensional Suzuki-phase lattice. This lattice was introduced in the context of sound propagation by sonic crystals [18]. Afterward, its equivalent for the case of dielectric rods in air was analyzed [19], and the corresponding made of holes in a dielectric slab studied [20], both showing interesting features for photonic bonding-antibonding states. In this work we show the calculated and experimentally measured photonic band structure of the Suzuki-phase of holes in dielectric. For the calculations we have used two dimensional plane expansion and three dimensional guided-mode expansion methods [21]. We find a wide bandgap (corresponding to the underlying triangular lattice of holes) that encloses two well-defined photonic bands with a very low group velocity along an entire specific direction of the reciprocal lattice. These photonic bands have been measured by angle-resolved photoluminescence (ARP). Defects have also been fabricated by removing some of the holes, forming microcavities. The defect states are clearly visible in the measurement by ARP of the photonic bands.

2. Theoretical analysis

Figure 1(a) shows the theoretical image of the Suzuki-phase structure. This structure is fabricated using a triangular lattice as reference and removing holes in order to create a rectangular lattice of missing holes. The periodicity is $2a$ in the Γ -X1 direction and $\sqrt{3}a$ in the Γ -X2 direction, where a is the lattice constant of the triangular lattice. The Brillouin zone is also shown in Fig. 1(b).

In Fig. 2 we show the two-dimensional photonic bands of the Suzuki lattice, taking the case of air holes with $r/a = 0.33$ in InP. Only even modes with respect to a horizontal mirror plane (usually called H or TE-like modes) are plotted. The interesting feature is the presence of two narrow photonic bands between $a/\lambda = 0.25$ and 0.3 . They originate from H_1 defects (i.e., a single missing hole in the triangular lattice) that are coupled in the rectangular structure to form weakly dispersive bands. In particular, the fifth band

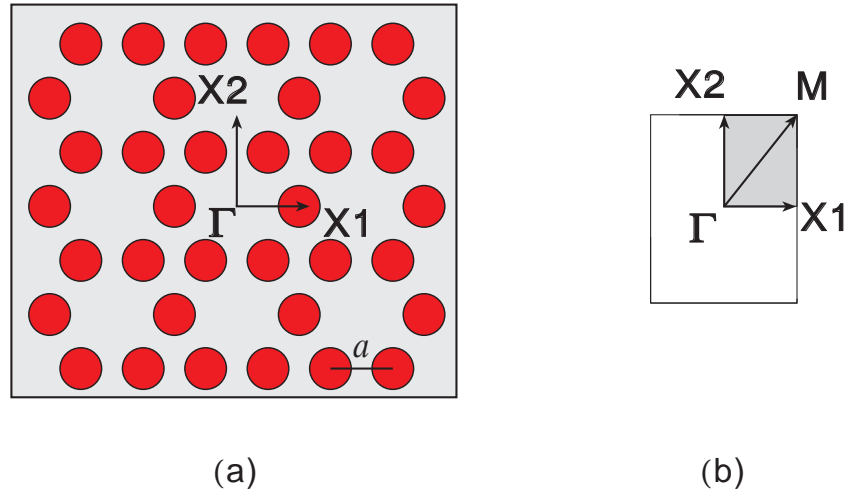


Fig. 1. (a) Theoretical image of the Suzuki structure. Arrows show the high symmetry directions. (b) Two-dimensional Brillouin zone with symmetry points.

is nearly flat along the Γ -X1 direction. This feature is important as it gives rise to a low-group velocity band.

The Suzuki lattice belongs to a set of 2D structures, like also the graphite and the Archimedean lattices, which possess a basis made of several rods per unit cell. All these lattices seem to support several low-dispersive photonic bands. A specific analogy between the Suzuki and the graphite lattice can be made, since both structures can be viewed as H_1 cavities that are coupled with supercell periodicity. Still, the Suzuki lattice has the unique feature of a nearly flat band along the whole Γ -X1 direction of the 2D Brillouin zone.

In order to calculate the photonic band dispersion of the InP-based structure used in the experiments, the vertical structure of the slab waveguide should be specified. We consider a slab waveguide made of a $d = 237$ nm thick InP core ($\epsilon = 10.1$) surrounded by a SiO₂ cladding ($\epsilon = 2.1$) on the lower side and by air ($\epsilon = 1$) on the upper side. The InP core layer is patterned with a Suzuki structure with a lattice constant $a = 455$ nm and hole radius $r/a = 0.33$. The photonic band dispersion is calculated with a guided-mode expansion method which consists of expanding the magnetic field on the bases of guided modes of an effective homogeneous waveguide with an average dielectric constant in each layer [21]. The results are shown in Fig. 3(a). As the slab waveguide is not symmetric with respect to a horizontal mirror plane, even (TE-like) and odd (TM-like) modes are coupled and give rise to a complex band structure. In particular, the presence of TM-like modes prevents opening of a complete photonic band gap for this structure. In order to analyze in a simpler way the experimental PL data, we calculate also a simplified form of the band structure in a “symmetric” approximation, which consists of taking identical lower and upper claddings with an average dielectric constant $\epsilon = 1.55$ (see Fig. 3(b)). Such slab is now symmetric and even (TE-like) modes can be defined. We notice that photonic bands are qualitatively similar to the 2D bands of Fig. 2, but they are blue-shifted due to vertical confinement in the slab waveguide.

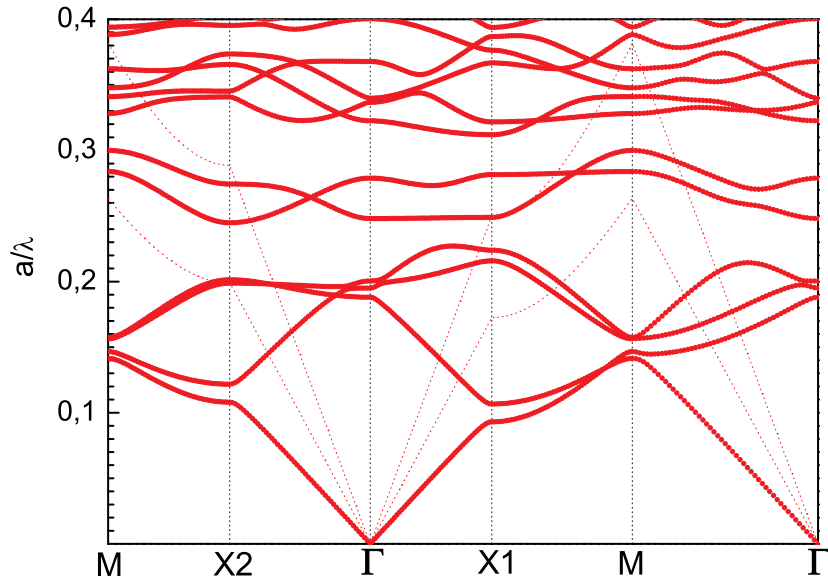


Fig. 2. Two dimensional simulations of the band diagram of the Suzuki-phase lattice. The parameters are $\epsilon = 10.1$ for the dielectric constant of the background material and $r/a = 0.33$ for the hole radius, where a is the lattice constant of the underlying triangular lattice. The “light lines” for air and silica claddings are drawn in red dashed lines.

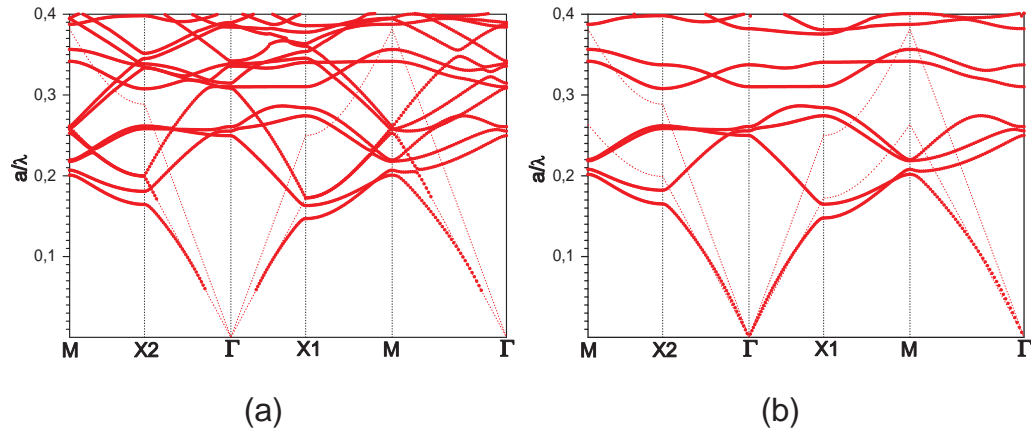


Fig. 3. Three dimensional simulations of the band diagram of the Suzuki lattice. Parameters are given in the text. (a) Full band structure of the air/InP/SiO₂ waveguide, (b) even (TE-like) modes of the “symmetric” waveguide where both upper and lower claddings have the same dielectric constant. The “light lines” for air and silica claddings are drawn in red dashed lines.

3. Experimental results

3.1. Band diagram of the Suzuki lattice

A 2D PC structure was fabricated on an InP slab incorporating an active medium with a total thickness of 237 nm. The heterostructure consists of four $In_{0.65}As_{0.35}P/InP$ quantum wells grown on an InP substrate by molecular beam epitaxy and it is transferred onto a silicon-on-silica substrate by wafer bonding (SiO_2 thickness = $0.9 \pm 0.1 \mu m$). The sample gives a strong luminescence in the range 1300-1700 nm. Standard techniques of electron-beam lithography and reactive ion-etching have been used for the patterning. Details on the fabrication procedure can be found elsewhere [22]. The Suzuki-phase lattices are fabricated on square areas with a lateral size of $25 \mu m$. Figure 4 shows the SEM image of the Suzuki-phase lattice.

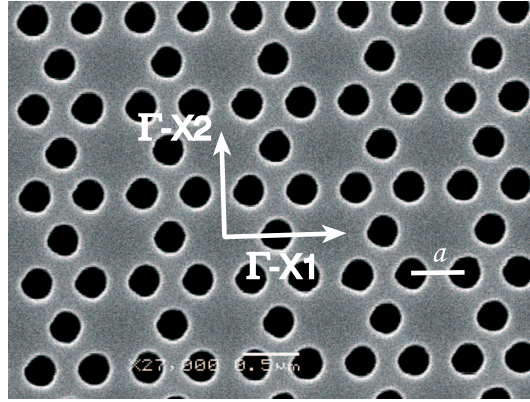


Fig. 4. SEM image of the fabricated Suzuki structure. The lattice parameter is $a = 455$ and the value of r/a is around 0.33. White arrows mark the directions that have been analyzed experimentally.

The sample was excited with a 635 nm laser diode through a $10\times$ (NA=0.26) objective placed at an angle of 45° with respect to normal incidence. The angle-revolved PL emission was collected by a fiber coupled to a Fourier-transform spectrometer (Bruker IFS66/s). An InGaAs p-i-n photodiode was used as a detector. The photoluminescence was collected at different angles with a resolution of ± 1 degree and these spectra were used to determine the photonic band dispersion through conservation of the wavevector parallel to the sample surface [23-26].

Figure 5 shows the PL spectra collected at $\theta = 0^\circ$ for the Suzuki-phase structure and for the unpatterned material. Two peaks related to the two isolated bands at the Γ point with normalized frequencies 0.315 and 0.342 (see Fig. 3(b)) can be clearly observed over the background. We have studied the angular dependence of the PL intensity for all the range between $\theta = 0^\circ$ to $\theta = 70^\circ$ (for higher angles no appreciable intensity was measured). Figures 6(a) and 6(b) show the PL intensity ratios as obtained by dividing the PL spectrum of the Suzuki-phase structure by the corresponding PL spectrum of the unpatterned area at the same emission angle, for two different directions of the 2D Brillouin zone. The energy of the observed maxima has been extracted and plotted in Fig. 6(c) as a function of wavevector, using conservation of momentum parallel to the surface. In the same figure we have included the 3D band calculated in the symmetric approximation for $a = 455 nm$, $r/a = 0.33$ and $d/a = 0.5209$.

A very good agreement between experiment and theory has been obtained. In the

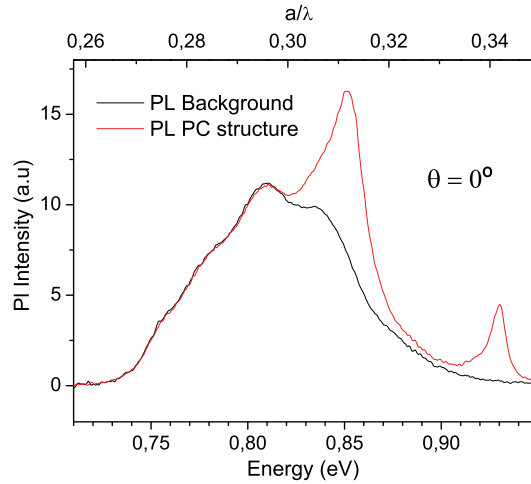


Fig. 5. Room-temperature photoluminescence spectra at $\theta = 0^\circ$ of the PC structure (red line) and of the unpatterned sample (black line).

Γ -X1 direction a very flat photonic band appears for energies around 0.85 eV. The slope in this region can take values down to $c/1000$. Experimentally, we have obtained values roughly below zero, around $-6 \times 10^{-3}c$ which indicates that light tends to concentrate along this direction of the reciprocal lattice. This strong decrease of the group velocity of the light traveling along this specific direction of the reciprocal lattice may have useful applications in photonic devices and sensors where non-confined light above the light cone may have a very strong interaction with substances deposited on the photonic crystal surface [14].

3.2. Defect Microcavity

We have also introduced intentional defects in the otherwise perfect Suzuki-phase lattice. A SP2 microcavity has been fabricated by removing two holes along the Γ -X2 direction (see SEM picture in inset of the Fig. 7(a)).

In order to analyze the effect of an SP2 microcavity we have measured the sample in two different configurations of the photoluminescence set-up. First, we have obtained the spectrum with an objective (0.65NA) placed perpendicular to the sample. We show the spectrum measured in this configuration in Fig. 7(a). The different peaks correspond to modes of the SP2 microcavity. Among all the peaks associated to the cavity, the peak around 0.8 eV (1.55 microns) presents the best quality factor ($Q_F \sim 120$) and it is located where the gain-absorption ratio reaches the maximum value [27].

The spectrum of the defect cavity in Fig. 7(a) has been used as a reference (it is worth to mention that an 0.65NA objective collects the emission of the sample in all directions from $\theta = 0^\circ$ to $\theta \sim 40^\circ$) in order to complement the measurements taken with the angle-resolved photoluminescence set-up. Indeed, once the energies of the defect modes are known, we can compare with the case of collecting the emission of the structure with the SP2 defect at 5° along the Γ -X1 direction. Figure 7(b) shows the spectra after normalizing with the background measured at the same emission angle for structures with and without defect (red and black lines respectively). In this case, the effect of the cavity is weaker as the emission is collected just around $5 \pm 1^\circ$ along the Γ -X1 direction. The inset of Fig. 7(b) shows clearly the effect of the cavity, corresponding

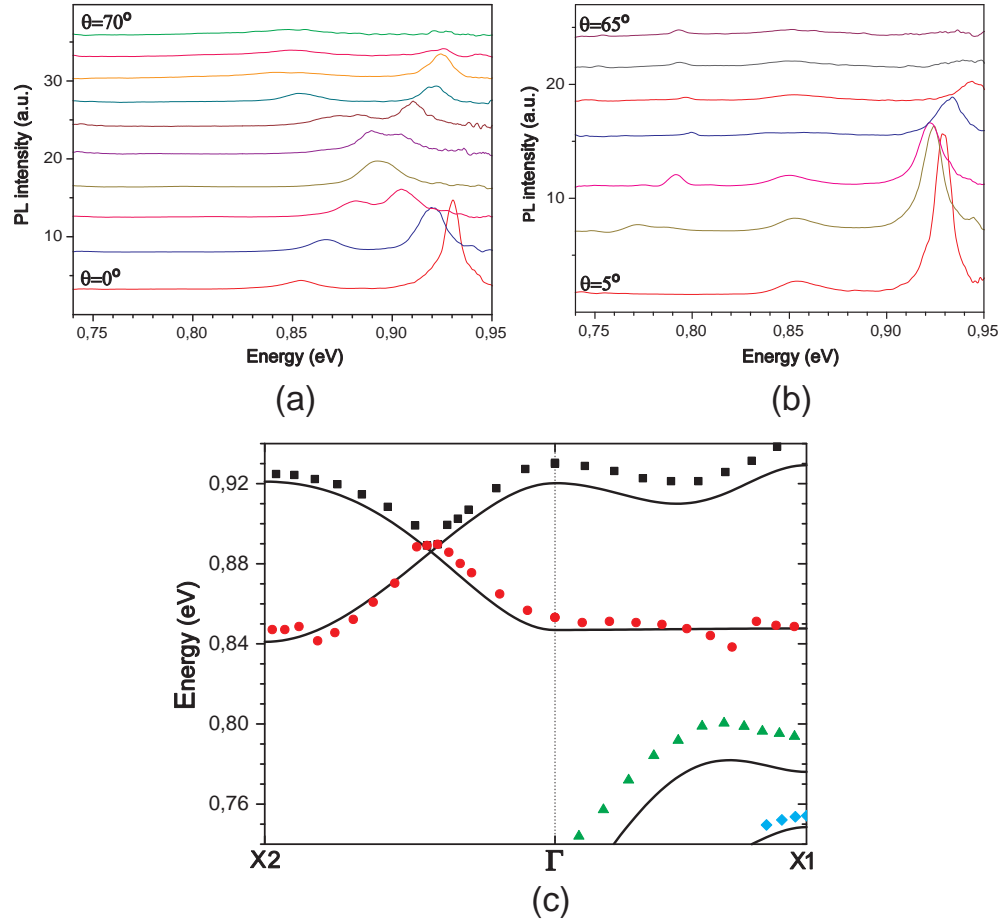


Fig. 6. (a) Normalized PL spectra in the X2- Γ direction for different angles ($\Delta\theta = 10^\circ$). Some extra spectra are plotted around the crossing in order to observe with higher accuracy the crossing point. (b) Normalized PL spectra in the Γ -X1 direction for different angles ($\Delta\theta = 10^\circ$). (c) Band diagram for the Suzuki lattice. Solid lines correspond to bands calculated by guided-mode expansion method with parameters $a = 455$ nm, $r/a = 0.33$ and $d/a = 0.5209$. Different shape and colors knots are the values obtained from the spectra measured by angle-resolved photoluminescence. At the crossing point, black squares and red circles are superimposed.

to the peak of higher quality factor of the same defect cavity measured with the non angle-resolved set-up. We therefore conclude that the cavity mode with $Q_F \sim 120$ at $\lambda = 1.55$ μm has a far field extending towards the normal direction.

In order to give a more complete analysis of the defect structures, we have calculated the cavity modes energies and Q-factors for the SP2 microcavity. We use again the guided-mode expansion [21] and introduce a SP2 defect with a 8×8 supercell repetition (i.e., 8 periods in both Γ -X1 and Γ -X2 directions). The frequencies of cavity modes are shown in Fig. 8(a) together with their Q-factors. In this calculation, the photonic bands of the periodic Suzuki-phase lattice are folded in a reduced Brillouin zone and their dispersion regions are indicated by grey areas. There are three cavity modes in the

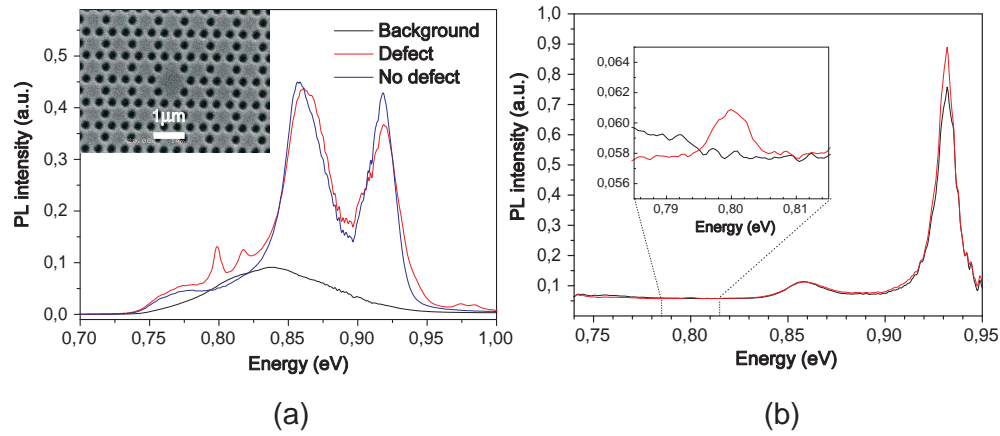


Fig. 7. (a) Spectra of unpatterned, defect and no defect structures (black, red and blue lines respectively) taken with an objective of 0.65NA at normal incidence. Inset: SEM image of the SP2 cavity on the Suzuki-phase lattice. (b) Normalized PL spectra measured at 5° for defect and no defect Suzuki-phase structure (red and black lines respectively). Inset: close-up view of the peak corresponding to the cavity mode.

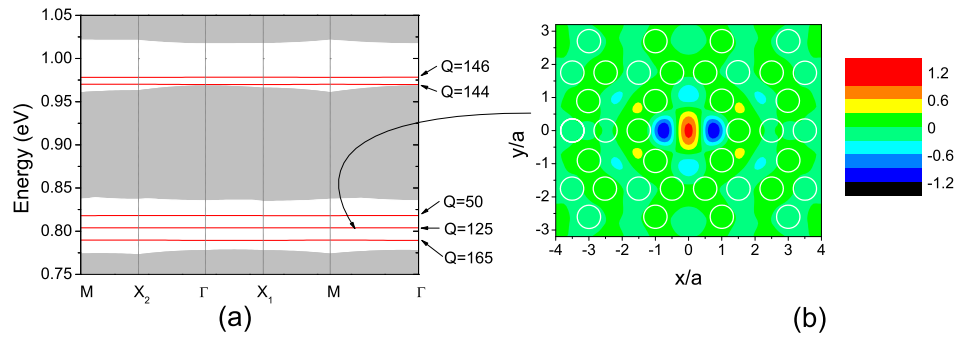


Fig. 8. (a) Cavity modes of the SP2 microcavity (in red) calculated with a 8×8 supercell. The Q-factors are indicated. The regions of the photonic bands of the periodic lattice folded in the 8×8 supercell are drawn by grey areas. (b) Contour plot of the H_z field component in the midplane of the InP slab, for the cavity mode with $Q=125$.

lowest photonic gap and two cavity modes in the upper gap. The modes with $Q=165$ and $Q=125$ might be tentatively assigned to the two peaks observed experimentally (see Fig. 7(a)). The measured quality factors are slightly lower than the calculated ones, which is reasonable in view of the presence of some disorder in the samples. The third mode with $Q=50$ might be hidden below the main peak corresponding to the band luminescence. The two modes at 0.97 - 0.98 eV can also be recognized in the experiment as a bump in the high-energy region, see again Fig. 7(a).

To illustrate the spatial properties of the cavity modes, we show in Fig. 8(b) a contour plot of the H_z field component calculated at a plane in the middle of the InP slab, for the mode with $Q=125$. The defect mode is strongly localized in the cavity region around the two missing holes. Note that the field has a maximum in the central position, it changes sign around $x = \pm 0.35a$, and it has an oscillatory behavior with side lobes at larger distances. The plot of Fig. 8(b) (and analogous ones for the other modes) demonstrate that the cavity modes are indeed localized states of the Suzuki-phase lattice with a SP2 microcavity.

4. Conclusion

We have determined the photonic band dispersion of the Suzuki-phase lattice realized in active InP-based slabs by theoretical calculations as well as by angle-resolved photoluminescence. Lateral sizes as small as $25\mu\text{m}$ have been measured. We have proven that the Suzuki-phase structure presents a quasi-flat band along the $\Gamma - X1$ direction which could be used as a slow light path through the sample. A very good agreement has been found between experimental and theoretical analysis of the band diagram. The presence of cavity modes in samples with defects is also established.

Low power intensity per area is needed to excite and measure the effect of intentional defects in the structure at different angles. Therefore, this method could be used to analyze with angular precision the conditions of laser emission, threshold and so on of structures which present higher quality factors.

Acknowledgments

A.R. Alija thanks an FPU fellowship AP2002-0474 and L.J. Martínez an I3P fellowship. The authors would also like to acknowledge support from European Network of Excellence IST-2-511616-NOE (PHOREMOST) and NMP4-CT-2004-500101 (SANDIE), Spain-Italy Integrated Action HI2004-0367/IT2304, projects NAN2004-08843-C05-04, TEC-2005-05781-C03-01, NAN2004-09109-C04-01, CONSOLIDER-Ingenio 2010 (CSD2006-00019), TEC2004-03545 and CARIPO Foundation.